



CO oxidation over Pd supported catalysts –*In situ* study of the electric and catalytic properties

V. Bratan, C. Munteanu, C. Horoiu*, A. Vasile, F. Papa, R. State, S. Preda, D. Culita, N.I. Ionescu

Institute of Physical Chemistry "Ilie Murgulescu" of the Romanian Academy – Splaiul Independenței 202, 060021 Bucharest, Romania

ARTICLE INFO

Article history:

Received 22 November 2016
Received in revised form 16 January 2017
Accepted 5 February 2017
Available online 6 February 2017

Keywords:

CO oxidation
Pd/SnO₂/TiO₂ and Pd/TiO₂ catalysts
Electrical conductivity

ABSTRACT

In this paper, the CO oxidation on Pd/TiO₂ and Pd/SnO₂/TiO₂ catalysts was studied using a non-conventional tool: AC electrical measurements in operando conditions. The structural and textural properties of the obtained powders have been characterized using BET, XRD, SEM, and CO chemisorption. Their redox properties were tested using the TPR technique. The surface dynamics was studied by electrical conductivity measurements under similar conditions with those encountered in the practical use in catalysis and correlated with their performances in CO oxidation.

© 2017 Elsevier B.V. All rights reserved.

1. Introduction

During the past several years a major attention was focused on the detection and removal of carbon monoxide, resulted from automotive emissions and industrial processes. The purpose of such research is to improve the quality of the environment. The catalytic oxidation is the main solution for the CO abatement. Many transition metal catalysts, such as Pd, Pt, Rh, and Au have been demonstrated to be very efficient in CO oxidation at low temperatures [1–5]. Noble metal catalysts usually require temperatures above 100 °C for efficient operation.

Pd-supported catalysts are used in commercial three-way catalysts, for CO and hydrocarbons oxidation, especially for that of methane [6–8]. Most Pd-containing catalysts used in CO oxidation have been supported on metal oxides, such as CeO₂, Co₃O₄, Mn₂O₃, SnO₂, and TiO₂ (Pd is one of the most active metals for interacting with the surface of oxides). The influence of the metal oxide support on the enhancement of the catalytic activity is well known and extensively studied [1,3,9,10].

Based on the previous studies, key factors that determine the behavior of the catalyst were found to be the oxygen storage capacity and the release properties of the support [11]. The competitive adsorption of CO and oxygen on Pd surface suppresses CO oxidation at lower temperatures [7]. The choice of a proper support that

activates oxygen improves the catalytic cycles. This is the case of Pd/CeO₂, Pd/TiO₂ and Pd/SnO₂ [12–14].

On the other hand, the contribution of the two controlling factors for the low-temperature oxidation of CO on Pd-supported catalysts are not sufficiently clarified, namely the valence state and the size of the metallic particles. Some studies considered that oxidized Pd plays the main role in the oxidation process, acting as an oxygen reservoir [8,15–17]. Other studies considered that the active phase in CO oxidation is the metallic Pd [18–21]. Anyway, a lower dispersion of Pd seems to be preferable for a higher activity, because highly dispersed Pd particles are easily oxidized but difficult to reduce them after [8,11].

The surface oxidation or reduction of semiconducting oxides-based catalysts could be investigated by following the evolution of the electrical properties of the solid in relation with a specific atmosphere. The surface conductivity may be increased or decreased by a chemisorbed substance. For example, in the case of n-type semiconductors, the surface conductivity is increased by electron transfer from a chemisorbed species to the solid (leading to a positively charged adsorbate) and decreased by electron transfer from solid surface to the adsorbate (leading to a negatively charged adsorbate). Thus, exposure to oxygen of an n-type semiconductor leads to the decrease of the conductivity with respect to that in an inert atmosphere, as a result of oxygen ions adsorption (the electron trapped by the adsorbed oxygen are provided by the surface of the oxide). On the contrary, the interaction with a reducing gas (such CO, H₂) results either in the formation of anion vacancies (acting as electron donors) or in the consumption of the oxygen ad-ions. Both

* Corresponding author.

E-mail address: chornoiu@icf.ro (C. Horoiu).

variants produce the increase of electron carrier concentration, so the increase of the conductivity. Thus, electrical conductivity measurements in operando conditions is a useful tool to investigate gas–solid electronic interactions and could be a good method for catalytic studies, permitting to follow the changes in the relative oxidation levels of the solid surface under reaction conditions [22–27].

In this work the AC electrical properties of Pd/TiO₂ and Pd/SnO₂/TiO₂ were studied in the temperature range of 30–400 °C, at atmospheric pressure and at a fixed frequency of 1592 Hz in order to determine the relative oxidation level of the surface. The catalytic properties of the samples were investigated in CO oxidation and correlated with the surface dynamics as resulted from electrical measurements.

2. Experimental

2.1. Materials and synthesis

The SnO₂/TiO₂ catalyst was obtained by impregnating TiO₂ (Rhône-Poulenc, S_{BET}-103 m²/g) with SnCl₄·5H₂O dissolved in ethanol, at room temperature. The amount of SnO₂ deposited on TiO₂ was calculated in order to obtain monolayer coverage (30% wt SnO₂). The sample was dried at 120 °C and then heated in air flow for 5 h at 500 °C. The TiO₂ support and the obtained sample were doped with 1% wt Pd, by impregnating them with palladium(II) acetate, Pd(OAc)₂, dissolved in acetone and treated again at 500 °C for 4 h after they have been dried at 120 °C [28].

2.2. Characterization

The samples were previously characterized by BET surface area measurements, X-ray diffraction and UV-vis diffuse reflectance spectroscopy [28]. In this paper, the samples were characterized by scanning electron microscopy (SEM), CO chemisorption and temperature programmed reduction (TPR).

The Pd dispersion and particle sizes were obtained using a ChemBET-3000 Quantachrome equipment, by CO chemisorption. Before analysis, the catalyst samples were flushed for 30 min in 5% H₂/Ar atmosphere (70 mL/min).

The morphology of the samples was investigated by scanning electron microscopy (SEM) using a high-resolution microscope, FEI Quanta 3D FEG model, operating at 20 kV, equipped with an energy dispersive X-ray (EDS) spectrometer, Apollo X. The analyses were done in a high vacuum, with Everhart–Thornley secondary electron (SE) detector.

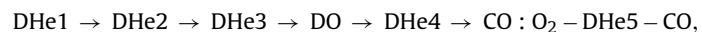
The temperature programmed reduction experiments (TPR) were performed on a ChemBET-3000 Quantachrome instrument equipped with thermal conductivity detector (TCD). The experiments were carried out by increasing the temperature from 298 K to 873 K at 10 K/min in a stream of 5% H₂/Ar (the flow rate being 70 mL/min). For keeping the stability and sensibility of measurements the H₂ concentration was obtained after the water formed during reduction was adsorbed onto a silicagel column. Before the beginning of the TPR measurements, the samples were flushed for 30 min at room temperature in a 5% H₂/Ar atmosphere.

2.3. Electrical conductivity measurements

The conductivity measurements were carried out as a function of temperature/atmosphere in operando conditions, using a reaction cell specially designed to allow the measurements in powder [29]. The catalyst (1.5 cm³) powder (fraction between 0.25 and 0.5 mm) was filling the annular space between the electrodes and was supported on a frit. The electrical conductivity, σ , was measured at 1592 Hz, in gas flow with an RLC bridge Hioki by using the

differential steps technique (DST) as described previously [22–24]. Under these conditions, the measured conductivity is dominated by surface conduction.

DST consists of successive heating (2°/5 °C/min heating rate between room temperature and 400 °C) and cooling (about 10 °C/min cooling rate) cycles in different gases, according to the protocol described below:



where DHe—dry helium (the numbers given above indicate the cycle number), DO—dry oxygen and CO:O₂—CO:O₂:He (4.75:4.75:91.5 molar ratio) and CO—CO:He (5:95 molar ratio). The gases used were research grade, 99.99% purity and dried using silicagel column. The total flow rate was 72 mL/min.

The conductivity data was commented by comparing plots in a specific cycle with those of the previous or the next one. Since the thermal cycling was performed in identical conditions and between the same limits, the information obtained indicates the effect of a certain atmosphere.

The content of inlet/exit gases was permanently monitored by gas chromatography (GC). Comparing the values obtained at the same temperature in different atmospheres allows correlating the electrical behavior of the semiconductor oxide with the changes occurred on the powder surface as a result of adsorption/desorption/catalytic reaction processes.

2.4. Catalytic data

The catalytic performances were evaluated during the CO: O₂ by periodically sampling the effluent into the gas chromatograph. The CO conversion was calculated based on the formula given as follows:

$$\text{conversion}(\%) = \frac{[\text{CO}]_{\text{in}} - [\text{CO}]_{\text{out}}}{[\text{CO}]_{\text{in}}} * 100 \quad (1)$$

where: [CO]_{out} represents the CO concentration after reaction (vol%) and [CO]_{in} – its initial concentration (vol%).

The obtained values, even if not absolute as in the case of stationary state data, are informative in terms of the trend of CO conversion.

The gas analysis was performed on-line with a GC (Pye, TCD detector) equipped with two parallel columns (Porapak Q and molecular sieves 5A) with helium as carrier gas.

3. Results and discussion

3.1. Characterization of the samples

Table 1 presents the studied samples with their abbreviations, BET surface areas (S_{BET}), the size of the particles and Pd dispersion.

As it can be seen, the surface area strongly decreased after impregnation with SnO₂ and Pd. The particle size of TiO₂ and Pd particle size are in the nanometric range and Pd dispersion is low and similar for the two compounds.

The major crystallographic phase observed for all samples is titanium dioxide in anatase form [28].

For Pd/TiO₂ sample the characteristic lines for oxidized Pd, PdO, were present (see **Fig. 1**). The diffraction peak at 33.9° can be indexed as (101) face of PdO nanoparticles [30]. The presence of oxidized palladium was expected because, although palladium acetate forms metallic Pd by decomposition, the samples were calcined in air at 500 °C and palladium starts to oxidize at temperatures above 350 °C [31]. For Pd/SnO₂/TiO₂ (not shown here) sample, supplementary diffraction peaks characteristic for tetragonal form in the SnO₂ structure appears [28]. This system presents a particular difficulty in identifying palladium oxide phase with XRD due to the

Table 1

The physicochemical characteristics of the samples (* - obtained from XRD, ** – obtained from CO chemisorption).

Sample	Abbreviation	S_{BET} (m^2/g)	Particle size of TiO_2 *	Pd dispersion (%)**	d_{Pd} (nm)**
TiO_2	TiO_2	103.0	16.5		
1% Pd/ TiO_2	Pd/ TiO_2	90.0	15.8	4.4	8.5
1% Pd/30% SnO_2/TiO_2	Pd/ SnO_2/TiO_2	55.1	13.2	5.3	6.9

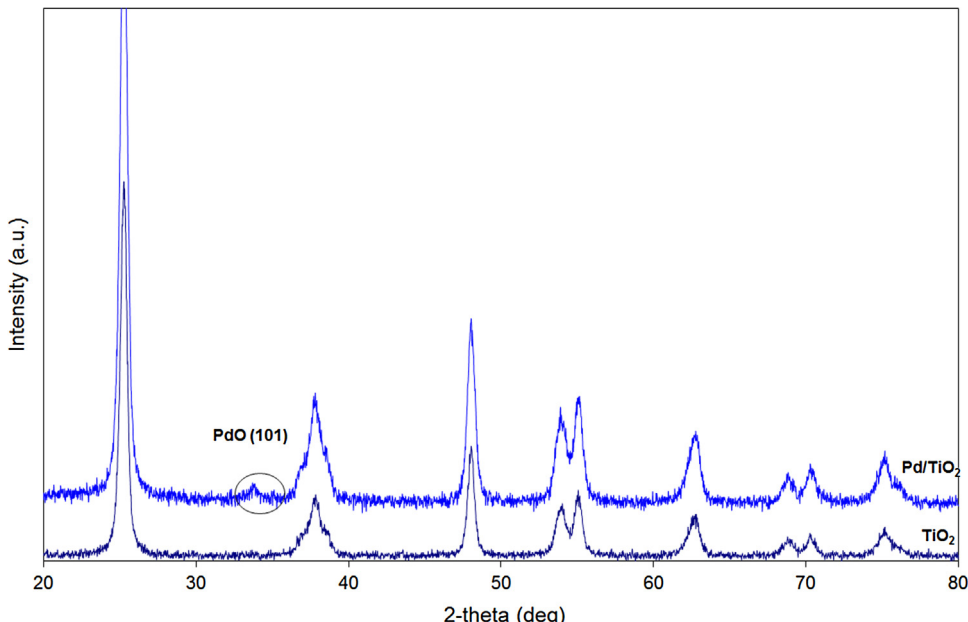


Fig 1. XRD spectra for Pd/TiO_2 .

overlap of the diffraction peak of PdO (101) with SnO_2 -cassiterite (101), which appears at 33.8° [32].

The SEM analysis presented in Fig. 2 for the Pd/TiO_2 sample indicate also the presence of small titania nanoparticles (<10 nm) with a low degree of crystallization having a very high tendency to agglomerate. The palladium nano-clusters were evidenced by the EDS and the backscattered electron detector analysis (Fig. 2b).

In the case of $Pd/SnO_2/TiO_2$ sample, the SEM analysis clearly showed the presence of the Pd nanoparticles on the SnO_2 crystallites (Fig. 3). This was also confirmed by the EDS analysis.

The UV-vis absorption spectra [28] confirm the presence of oxidized Pd. A broad band between 400 and 500 nm centered at 470 nm was obtained, assigned to d-d transition in PdO particles [33,34].

The reducibility of the samples was studied by using H_2 -TPR and the corresponding profiles of the reduction up to $750^\circ C$ are presented in Fig. 4.

H_2 -TPR of TiO_2 shows a high-temperature peak (around $570^\circ C$), which is ascribed to the reduction of the surface Ti^{4+} ions [35]. The containing Pd samples present a similar peak at about $340^\circ C$, attributed also to the TiO_2 surface reduction. The Pd addition increases the reducibility of the support, so the temperature of the reduction decreases. For $Pd/SnO_2/TiO_2$ a much pronounced H_2 consumption appears at high temperature, due to the Sn^{4+} - Sn^{2+} reduction [36].

The negative peak observed around $70^\circ C$ in the H_2 -TPR of Pd/TiO_2 is attributable to decomposition of palladium β -hydride formed by palladium with H_2 at room temperature during the pre-treatment at the beginning of the analysis [37]. When the system was exposed to hydrogen the reduction of palladium oxide takes place, followed by hydrogen chemisorption, maybe hydrides formation. On heating, the H_2 production takes place due to the

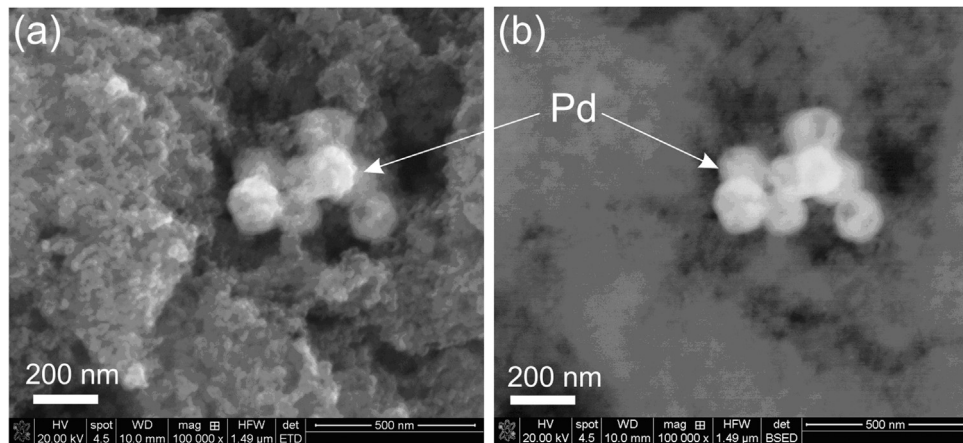
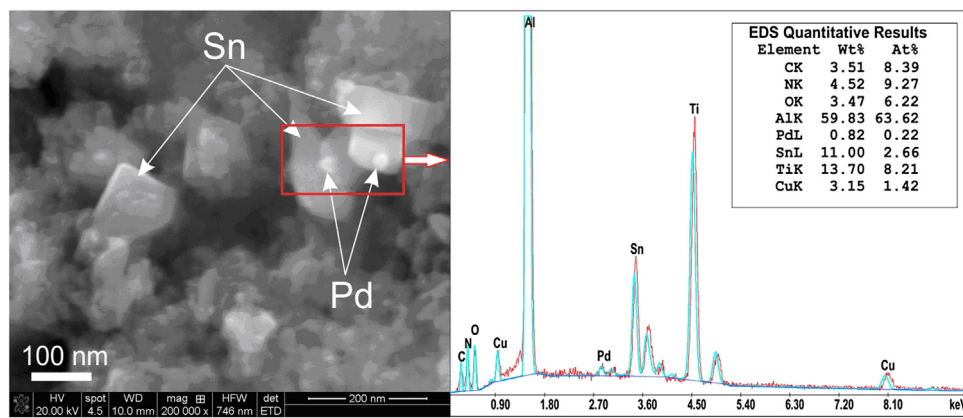
desorption of hydrogen/decomposition of hydrides. It is known that the tendency to form hydride phase increases with increasing Pd dispersion [38]. The presence of this peak doesn't exclude the presence of the oxidized Pd because its reduction (the Pd^{2+} - Pd^0 transition) could take place even at room temperature in reducing atmosphere during the pre-treatment [10,39,40].

In the case of $Pd/SnO_2/TiO_2$, the negative peak is weaker. On the other hand, in this case, a positive peak around $150^\circ C$ is observed, which may be attributed to the PdO surface reduction, as it was also reported for PdO supported on different oxides [41,42]. The only difference between the two catalysts is the presence of SnO_2 in the $Pd/SnO_2/TiO_2$ sample. So it could be concluded that SnO_2 stabilizes the oxidized form of Pd due to the SMSI (Strong Metal Support Interaction) effect [43,44].

3.2. Electrical characterization

Understanding conductivity data is not easy since the total conductivity is, in a simplified matter, the sum of ionic and electronic conductivity. In the temperature range used in this study (30 – $400^\circ C$), the electronic conductivity prevails, due to a much smaller size, implying a much higher mobility of these carriers. Consequently, the conductivity results are discussed in terms of electron transfer.

Fig. 5 presents the Arrhenius dependence of the electrical conductivity for Pd/TiO_2 and $Pd/SnO_2/TiO_2$ catalysts. As already mentioned in the experimental part, the measured conductivity is dominated by the surface conduction. The conductivity measurements were performed *in operando* conditions starting with three heating-cooling cycles in helium flow (DHe1-3), used to clean the surface from the atmospheric contaminants. It can be observed that the values of the electrical conductivity in DHe2 and DHe3 runs

Fig. 2. SEM images of the Pd/TiO₂ sample.Fig. 3. SEM and EDS analysis of the Pd/SnO₂/TiO₂ sample (the Al and Cu signals comes from the support stub).

are almost identical in high-temperature range, indicating a good stability of the surface. The higher values obtained in DHe1 (the first flushing in dry helium atmosphere) was due to desorption of contaminants (especially water) [22,45].

For the studied samples lower conductivity values were obtained when flushing in oxygen atmosphere (DO runs) with respect to the values measured in the helium atmosphere (DHe3), indicating them as n-type semiconductors. This behavior can be attributed to the presence of oxygen vacancies or to the presence of cationic sites Ti³⁺ acting as electron donors.

Special patterns of the electrical conductivity variation with temperature were obtained for Pd-containing samples in helium runs. A conductivity maximum was obtained around 200 °C (1000/T = 2.11). The increase of conductivity in the case of an n-type semiconductor can be associated with a surface reduction, most probably due in this case to palladium oxide reduction since this was not observed for the support (not shown here). The temperature corresponding to the maximum of the conductivity (considered to be the temperature necessary for PdO reduction) was higher than in the TPR experiments. This happens because the samples were flushed in an inert atmosphere that acts like a weaker reducing agent (the loss of oxygen by repeated inert flushing is equivalent to a slight reduction) than hydrogen. On the other hand, the peak obtained for Pd/SnO₂/TiO₂ sample was less pronounced, which can be explained by the stabilization of the oxidized form of Pd in the presence of SnO₂, as resulted also from TPR experiments. A decrease of surface conductivity follows in the temperature range 200–250 °C, associated with the regeneration of PdO structure [45] probably due to the diffusion of bulk oxygen, while is no oxygen in

the surrounding atmosphere. Starting at 250 °C (1000/T = 1.91), the samples show a normal semiconductor behavior (an exponential increase of conductivity with temperature) that can be attributed to the existence of oxygen vacancies in TiO₂ lattice.

During the catalytic testing (CO:O₂ 1:1 molar ratio) the variation of conductivity with temperature was similar in cases of Pd/TiO₂ and Pd/SnO₂/TiO₂ samples, but strongly different from the support (Fig. 6). The conductivity increases up to 150 °C and has higher values than in corresponding DO run.

Comparing the variation of conductivity in the two cycles: DO and CO:O₂ and considering the n-type behavior of the samples, it could be supposed that the process below 150 °C (1000/T = 2.36) must be related to PdO reduction by the interaction with CO. After this temperature, the conductivity decreases tending to attain the values obtained for the oxidized sample. This behavior is connected with oxygen chemisorption and the regeneration of the PdO structure, as it was reported before for PdO/BN catalysts [45].

In order to determine the ability of the samples to donate the oxygen of the lattice, it was measured the variation of conductivity with temperature when flushing in reducing atmosphere. In Fig. 7 were presented the Arrhenius plots for catalyst samples flushing in a CO: He mixture (CO run). Pd-containing samples were very sensitive to the presence of CO in absence of oxygen. In the figure one can see the presence of various regions where the conductivity increases linearly, differentiated by the slope, due to the ionization of various electronic levels located deeper in the forbidden band. The very sharp increase in the conductivity could be ascribed to the adsorption of CO followed by a surface reduction, meaning the consumption of surface oxygen for the CO oxidation. This affir-

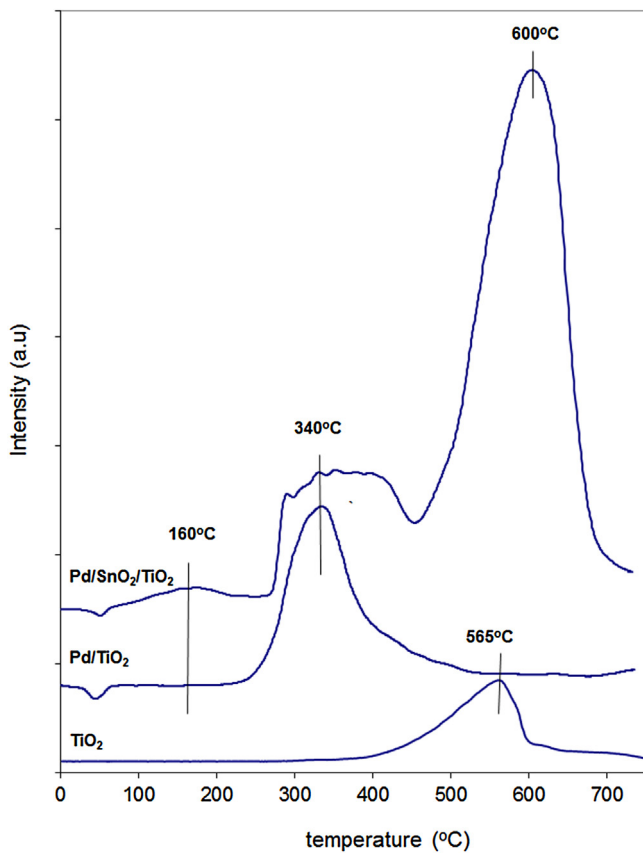


Fig. 4. Temperature programmed reduction (TPR) of TiO_2 , Pd/TiO_2 and $\text{Pd/SnO}_2/\text{TiO}_2$.

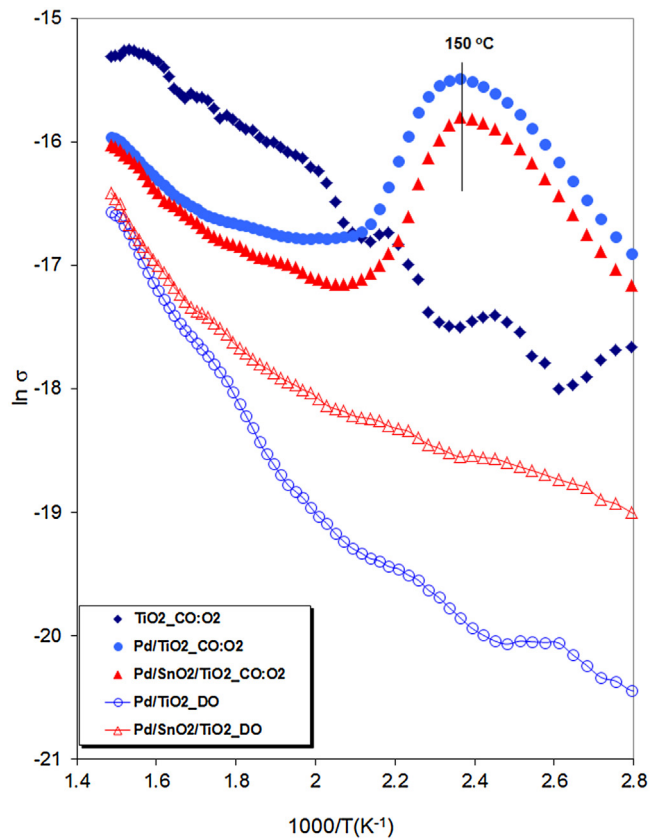


Fig. 6. Arrhenius dependence of conductivity measured in operando conditions during the catalytic test (CO:O_2 1:1) for TiO_2 , Pd/TiO_2 and $\text{Pd/SnO}_2/\text{TiO}_2$. The variation of conductivity on heating in dry oxygen (DO) was presented for comparison.

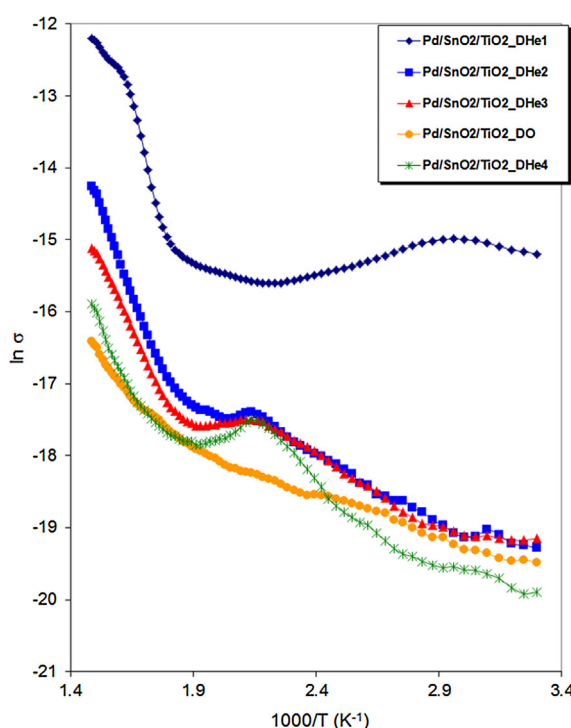
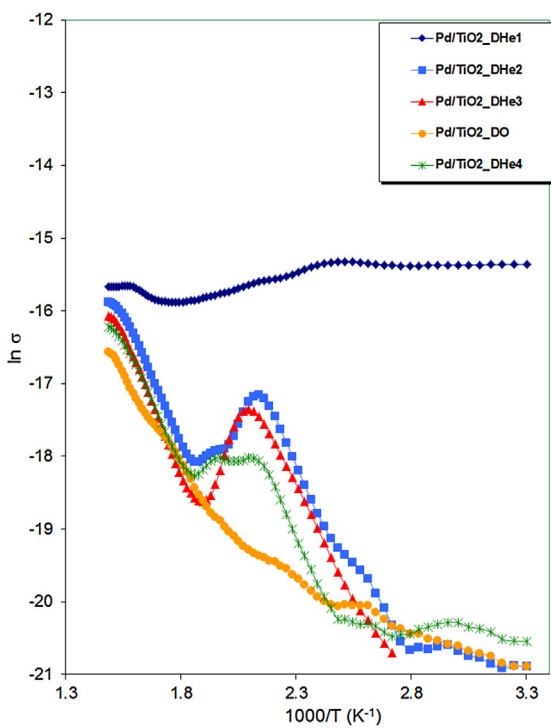


Fig. 5. The Arrhenius dependence of conductivity σ (measured in $\text{ohm}^{-1} \cdot \text{m}^{-1}$) for: a) Pd/TiO_2 and b) $\text{Pd/SnO}_2/\text{TiO}_2$ samples on heating in dry helium DHe1-4 and in dry oxygen – DO.

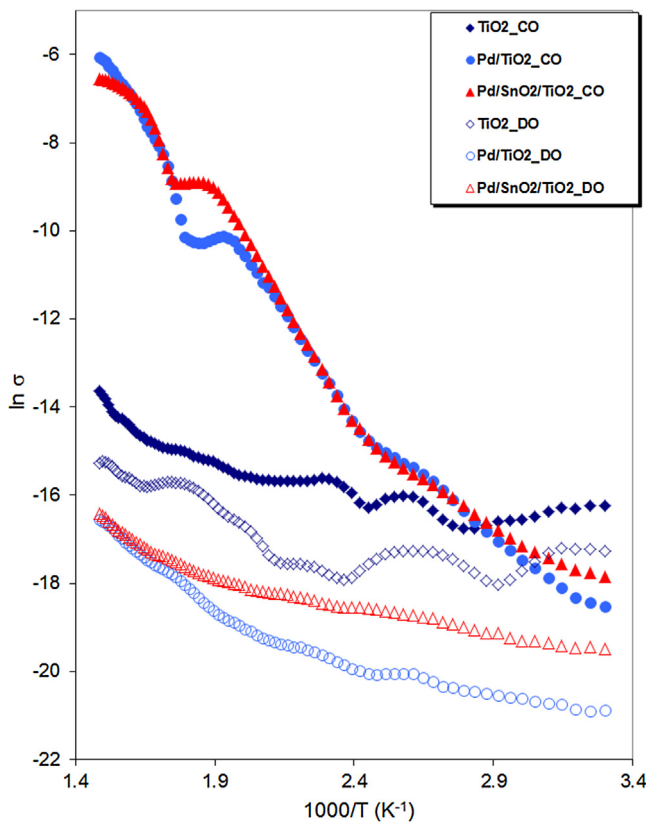


Fig. 7. The conductivity variation (measured in $\text{ohm}^{-1} \cdot \text{m}^{-1}$) in CO:He run for TiO_2 , Pd/TiO_2 and $\text{Pd/SnO}_2/\text{TiO}_2$.

Table 2

The apparent activation energy of conduction for studied catalysts in different atmospheres calculated in the temperature range 300–400 °C.

Sample	DHe3	DO	CO:O ₂	CO:He
TiO_2	0.6	0.3 ^a	0.2 ^b	0.5
Pd/TiO_2	0.5	0.4	0.3	1.1
$\text{Pd/SnO}_2/\text{TiO}_2$	0.6	0.3	0.3	1.1

^a 330–400 °C.

^b 280–380 °C.

mation is sustained by the fact that CO_2 is obtained in the outlet gas at temperatures above 50 °C (not presented here). By CO_2 desorption the free electrons associated with the reduced Pd/Ti sites are released into the conduction band of the solid, resulting in the increase of conductivity. The TiO_2 support behavior is completely different because the conductivity increases very slowly comparing with the values obtained in presence of oxygen. This is due to the low reducibility of TiO_2 in the studied temperature range. As resulted also from TPR data, the addition of Pd strongly increases the reducibility of the support.

The electrical conductivity (σ) of all samples follows the Arrhenius law: $\sigma = \sigma_0 \exp\left(-\frac{E_c}{kT}\right)$, where σ_0 is a pre-exponential factor, E_c is the apparent activation energy of conduction, k – the Boltzmann constant and T – the absolute temperature. The apparent activation energies of conduction in the high-temperature range (above 300 °C) were calculated from the slope of the straight line of this region of the $\ln(\sigma)$ versus $1000/T$ plots (Figs. 5–7) and summarized in Table 2. In this temperature range, the conductivity is determined mainly by the support, making it possible to compare the behavior of the samples in different atmospheres based on the values of activation energy.

The results indicate that are at least three surface states with the energy level of ~0.3, 0.6 and 1 eV respectively. The activation

energies of conduction for Pd-containing samples in presence of He or oxygen are similar with the activation energies for TiO_2 . This is expected because the support dictates the electrical properties of the surface [22,23].

The activation energy in a dry inert atmosphere for all samples is ~0.6 eV, lower than 1.6 eV, which is half the band gap of the anatase. The difference can be explained considering the presence of shallow donor levels which narrow the gap between the valence and the conduction bands. Because the working temperature is reduced, the conduction mechanism is supposed to be an electronic type and the lower values of activation energy (0.3 and 0.6 eV) are ascribed to the presence of the oxygen vacancies. Similar values have been reported before for the anatase in similar conditions [46,47].

Flowing in the CO:O₂ mixture the conduction activation energy of catalysts are similar with the values obtained in dry oxygen run and lower than the values obtained in dry inert. The results suggest an oxidized surface in presence of catalytic mixture, at temperatures higher than 300 °C.

In CO:He flow (reducing atmosphere) for Pd-containing samples a new surface state appears. This state is assigned to Ti^{4+} – Ti^{3+} reduction [47], sustaining the sharp increase of conductivity in CO:He run. Once again, the conductivity data are in agreement with the TPR results: Pd addition strongly increases the reducibility of the TiO_2 support.

3.3. Catalytic performances

It is generally accepted that CO oxidation on the supported noble metal catalysts proceeds *via* a Langmuir–Hinshelwood (L–H) reaction, between adsorbed CO and dissociatively adsorbed oxygen, metallic Pd being assigned as the active species [3,19]. The conversion is generally reduced at lower temperatures because CO is strongly adsorbed on Pd, resulting in unavailability of the oxygen activation [48].

Fig. 8 presents the CO oxidation activity of the Pd-containing samples in the temperature range 30–400 °C. As a comparison, CO oxidation over the TiO_2 support was also performed under the same conditions and was also shown. As it can be seen the support shows no CO oxidation activity up to 350 °C.

It should be noted that the palladium-containing catalysts are able to convert CO to CO_2 at low temperatures, although the molar ratio CO:O₂ is 1:1. The CO conversion on Pd/TiO_2 and $\text{Pd/SnO}_2/\text{TiO}_2$ samples increases gradually with the temperature increase. The low concentration of active sites results in the S-shaped behavior of the light-off curves.

At lower temperatures, $\text{Pd/SnO}_2/\text{TiO}_2$ sample presents higher activity: the conversion is 61.4% at 165 °C while for Pd/TiO_2 the conversion is just 45.2%. This difference in the activity of the two samples couldn't be explained by the surface area or dispersion of Pd ($\text{Pd/SnO}_2/\text{TiO}_2$ has lower surface area and the Pd dispersion is similar for the two samples). Taking into account the conclusions resulted from TPR and electrical measurements, the increased conversion at low temperature is correlated to the reduction of PdO to Pd. The higher conversion is obtained in the case of $\text{Pd/SnO}_2/\text{TiO}_2$ sample because SnO_2 stabilizes Pd in the oxidized state.

The presence of PdO on the surface modifies the behavior of the catalysts at low temperatures by the emergence of another reaction path, namely: the CO strongly adsorbed on metallic Pd reacts with oxygen from PdO, similar with the mechanism proposed for methane oxidation [8]. The PdO reduction is reflected in the pronounced rising of the conduction up to 150 °C, comparing with oxidized sample (Fig. 6):



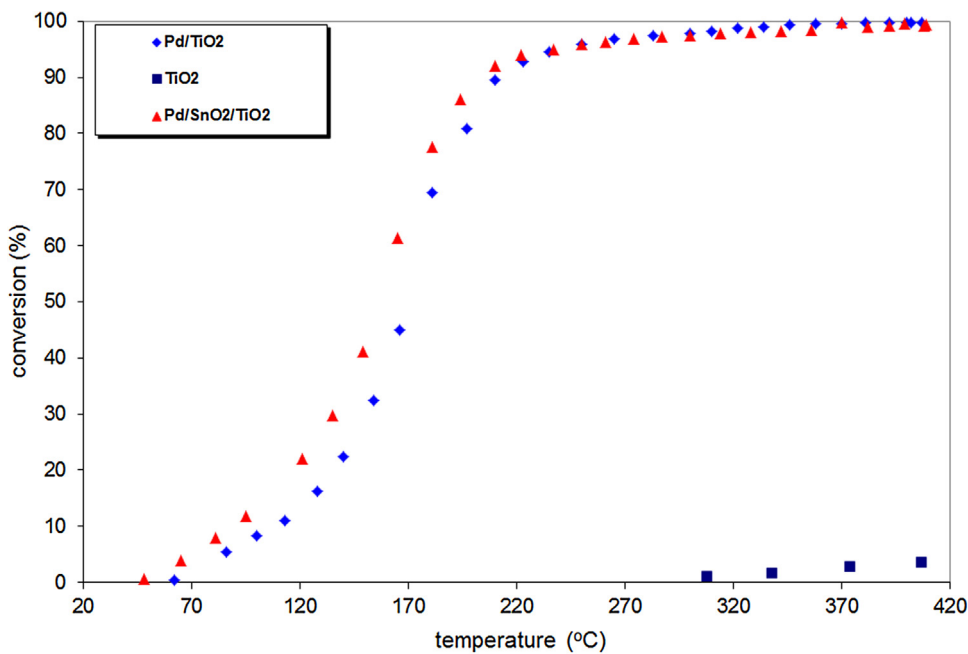
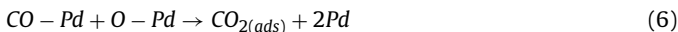


Fig. 8. CO conversion measured for TiO₂, Pd/TiO₂ and Pd/SnO₂/TiO₂ catalysts.

Above this temperature, the reaction takes place mainly between the adsorbed CO on Pd and the surface oxygen from PdO. At temperatures higher than 150 °C, the Pd is totally reduced and the strength of Pd-CO bonding decreases permitting the oxygen adsorption.



The CO oxidation proceeds over a typical Langmuir-Hinshelwood mechanism. This is confirmed by the variation of conduction with temperature. Thus, above 150 °C a conduction drop of the samples in CO:O₂ atmosphere occurs, then the values approach those obtained in presence of O₂ when the sample is supposed to be completely oxidized (at higher temperatures the apparent activation energies of conduction of the two cycles are equal).

Additionally, the reducibility of TiO₂ increases with temperature and the support could provide the oxygen from the reaction. Consequently, the conversion increases significantly.

4. Conclusions

In this study, the CO oxidation on some Pd-supported catalysts was studied using a non-conventional tool: AC electrical measurements in operando conditions. This technique when adequately used is an expedient method for determining the modification in the oxidation state of the catalyst during the reaction. The physicochemical properties of the samples and their performances in CO oxidation reactions were correlated in order to detect the nature of the active sites.

When Pd was impregnated on TiO₂ and SnO₂/TiO₂ the catalytic performances of obtained samples were increased.

At lower temperatures, the CO conversion is related to the presence of the palladium oxide (PdO). Because of the stabilization of PdO form, the palladium supported on SnO₂/TiO₂ showed enhancement for lower temperature activity.

At temperatures higher than 200 °C the CO conversion was nearly 100%. When the temperature increases the PdO was totally reduced but in the same time, the Pd-CO bonding energy decreases permitting the oxygen activation.

Acknowledgements

This research was made under the finance support by PN-II UEFISCDI, grant INTEGRATREAT 100/2012. The authors gratefully acknowledge the support of the EU (ERDF) and Romanian Government, which allowed for acquisition of the research infrastructure under POS-CCE O 2.2.1 project INFRANANOCHEM - Nr. 19/01.03.2009.

References

- [1] L. Liu, F. Zhou, L. Wang, X. Qi, F. Shi, Y. Deng, Low-temperature CO oxidation over supported Pt, Pd catalysts: particular role of FeO_x support for oxygen supply during reactions, *J. Catal.* 274 (2010) 1–10.
- [2] B. Kalita, R.C. Deka, Reaction intermediates of CO oxidation on gas phase pd4 clusters: a density functional study, *J. Am. Chem. Soc.* 131 (2009) 13252–13254.
- [3] R.V. Gulyaev, A.I. Stadnichenko, E.M. Slavinskaya, A.S. Ivanova, S.V. Koscheev, A.I. Boronin, In situ preparation and investigation of Pd/CeO₂ catalysts for the low-temperature oxidation of CO, *Appl. Catal. A: Gen.* 439–440 (2012) 41–50.
- [4] M. Haruta, N. Yamada, T. Kobayashi, S. Iijima, Gold catalysts prepared by coprecipitation for low-temperature oxidation of hydrogen and of carbon monoxide, *J. Catal.* 115 (1989) 301–309.
- [5] P. Granger, V.I. Parvulescu, Catalytic NO_x Abatement systems for mobile sources: from three-way to lean burn after-treatment technologies, *Chem. Rev.* 111 (2011) 3155–3207.
- [6] B.E. Nieuwenhuys, The surface science approach toward understanding automotive exhaust conversion catalysis at the atomic level, in: B.C.G. Werner, O. Haag, K. Helmut (Eds.), *Advances in Catalysis*, Academic Press, 1999, pp. 259–328.
- [7] A. Satsuma, K. Osaki, M. Yanagihara, J. Ohyama, K. Shimizu, Activity controlling factors for low-temperature oxidation of CO over supported Pd catalysts, *Appl. Catal. B: Environ.* 132–133 (2013) 511–518.
- [8] K.-I. Fujimoto, F.H. Ribeiro, M. Avalos-Borja, E. Iglesia, Structure and reactivity of PdO_x/ZrO₂ catalysts for methane oxidation at low temperatures, *J. Catal.* 179 (1998) 431–442.
- [9] B. Wang, D. Weng, X. Wu, J. Fan, Influence of H₂/O₂ redox treatments at different temperatures on Pd-CeO₂ catalyst: structure and oxygen storage capacity, *Catal. Today* 153 (2010) 111–117.
- [10] H. Zhu, Z. Qin, W. Shan, W. Shen, J. Wang, Low-temperature oxidation of CO over Pd/CeO₂-TiO₂ catalysts with different pretreatments, *J. Catal.* 233 (2005) 41–50.

[11] A. Satsuma, K. Osaki, M. Yanagihara, J. Ohyama, K. Shimizu, Low temperature combustion over supported Pd catalysts –strategy for catalyst design, *Catal. Today* 258 (Part 1) (2015) 83–89.

[12] M. Jin, J.-N. Park, J.K. Shon, J.H. Kim, Z. Li, Y.-K. Park, J.M. Kim, Low temperature CO oxidation over Pd catalysts supported on highly ordered mesoporous metal oxides, *Catal. Today* 185 (2012) 183–190.

[13] M. Fernández-García, A. Martínez-Arias, L.N. Salamanca, J.M. Coronado, J.A. Anderson, J.C. Conesa, J. Soria, Influence of ceria on Pd activity for the CO + O₂ reaction, *J. Catal.* 187 (1999) 474–485.

[14] H. Zhu, Z. Qin, W. Shan, W. Shen, J. Wang, CO oxidation at low temperature over Pd supported on CeO₂–TiO₂ composite oxide, *Catal. Today* 126 (2007) 382–386.

[15] H. Yoshida, T. Nakajima, Y. Yazawa, T. Hattori, Support effect on methane combustion over palladium catalysts, *Appl. Catal. B: Environ.* 71 (2007) 70–79.

[16] S. Colussi, A. Trovarelli, E. Vesselli, A. Baraldi, G. Comelli, G. Groppi, J. Llorca, Structure and morphology of Pd/Al₂O₃ and Pd/CeO₂/Al₂O₃ combustion catalysts in Pd–PdO transformation hysteresis, *Appl. Catal. A: Gen.* 390 (2010) 1–10.

[17] H. Gabasch, A. Knop-Gericke, R. Schlogl, M. Borasio, C. Weilach, G. Rupprechter, S. Penner, B. Jenewein, K. Hayek, B. Klotzer, Comparison of the reactivity of different Pd–O species in CO oxidation, *Phys. Chem. Chem. Phys.* 9 (2007) 533–540.

[18] M. Lyubovsky, L. Pfefferle, Complete methane oxidation over Pd catalyst supported on α -alumina. Influence of temperature and oxygen pressure on the catalyst activity, *Catal. Today* 47 (1999) 29–44.

[19] L.-Y. Jin, J.-Q. Lu, X.-S. Liu, K. Qian, M.-F. Luo, Thermal stable Pd/Ce_{0.2}Y_{0.8}O_{2-δ} catalysts for CO and CH₄ oxidation, *Catal. Lett.* 128 (2009) 379–384.

[20] S.K. Kulshreshtha, M.M. Gadgil, Physico-chemical characteristics and CO oxidation studies over Pd/(Mn₂O₃ + SnO₂) catalyst, *Appl. Catal. B: Environ.* 11 (1997) 291–305.

[21] T. Schalow, B. Brandt, M. Laurin, S. Schauermann, J. Libuda, H.J. Freund, CO oxidation on partially oxidized Pd nanoparticles, *J. Catal.* 242 (2006) 58–70.

[22] M. Caldăraru, G. Postole, C. Horoianu, V. Bratan, M. Dragan, N.I. Ionescu, Electrical conductivity of γ -Al₂O₃ at atmospheric pressure under dehydrating/hydrating conditions, *Appl. Surf. Sci.* 181 (2001) 255–264.

[23] M. Caldăraru, C. Munteanu, P. Chesler, M. Carata, C. Horoianu, N.I. Ionescu, G. Postole, V. Bratan, Supported oxides as combustion catalysts and as humidity sensors. Tuning the surface behavior by inter-phase charge transfer, *Microporous Mesoporous Mater.* 99 (2007) 126–131.

[24] M. Caldăraru, M. Scurtu, C. Horoianu, C. Munteanu, T. Blasco, J.M. López Nieto, Electrical conductivity of a MoVTeNbO catalyst in propene oxidation measured in operando conditions, *Catal. Today* 155 (2010) 311–318.

[25] I. Popescu, Y. Wu, P. Granger, I.-C. Marcu, An in situ electrical conductivity study of LaCoFe perovskite-based catalysts in correlation with the total oxidation of methane, *Appl. Catal. A: Gen.* 485 (2014) 20–27.

[26] J.-M. Herrmann, The electronic factor and related redox processes in oxidation catalysis, *Catal. Today* 112 (2006) 73–77.

[27] Y. Maeda, Y. Iizuka, M. Kohyama, Generation of oxygen vacancies at a Au/TiO₂ perimeter interface during CO oxidation detected by in situ electrical conductance measurement, *J. Am. Chem. Soc.* 135 (2013) 906–909.

[28] M. Caldăraru, D. Spîrneanca, V.T. Popa, N.I. Ionescu, Surface dynamics in tin dioxide-containing catalysts II. Competition between water and oxygen adsorption on polycrystalline tin dioxide, *Sens. Actuators B: Chem.* 30 (1996) 35–41.

[29] V. Bratan, C. Munteanu, P. Chesler, D. Negoeșcu, N.I. Ionescu, Electrical characterization and the catalytic properties of SnO₂/TiO₂ catalysts and their Pd-supported equivalents, *Rev. Roum. Chim.* 59 (2014) 335–341.

[30] H. Lorenz, Q. Zhao, S. Turner, O.I. Lebedev, G. Van Tendeloo, B. Klötzer, C. Rameshan, K. Pfaller, J. Konzett, S. Penner, Origin of different deactivation of Pd/SnO₂ and Pd/GeO₂ catalysts in methanol dehydrogenation and reforming: a comparative study, *Appl. Catal. A: Gen.* 381 (2010) 242–252.

[31] S. Penner, D. Wang, B. Jenewein, H. Gabasch, B. Klötzer, A. Knop-Gericke, R. Schlogl, K. Hayek, Growth and decomposition of aligned and ordered PdO nanoparticles, *J. Chem. Phys.* 125 (2006) 094703.

[32] W.H. Baur, Über die Verfeinerung der Kristallstrukturbestimmung einiger Vertreter des Rutiltyps: TiO₂ SnO₂, GeO₂ und MgF₂, *Acta Crystallogr.* 9 (1956) 515–520.

[33] Z. Zhang, G. Mestl, H. Knözinger, W.M.H. Sachtle, Effects of calcination program and rehydration on palladium dispersion in zeolites NaY and 5A, *Appl. Catal. A: Gen.* 89 (1992) 155–168.

[34] D. Tessier, A. Rakai, F. Bozon-Verduraz, Spectroscopic study of the interaction of carbon monoxide with cationic and metallic palladium in palladium–alumina catalysts, *J. Chem. Soc. Faraday Trans.* 88 (1992) 741–749.

[35] V.G. Deshmane, S.L. Owen, R.Y. Abrokwh, D. Kuila, Mesoporous nanocrystalline TiO₂ supported metal (Cu, Co, Ni, Pd, Zn, and Sn) catalysts: effect of metal–support interactions on steam reforming of methanol, *J. Mol. Catal. A: Chem.* 408 (2015) 202–213.

[36] R. Sasikala, N.M. Gupta, S.K. Kulshreshtha, Temperature-programmed reduction and CO oxidation studies over Ce–Sn mixed oxides, *Catal. Lett.* 71 (2001) 69–73.

[37] D.A. Papaconstantopoulos, B.M. Klein, E.N. Economou, L.L. Boyer, Band structure and superconductivity of PdD_x and Pd_x, *Phys. Rev. B* 17 (1978) 141–150.

[38] C.M. Mendez, H. Olivero, D.E. Damiani, M.A. Volpe, On the role of Pd β -hydride in the reduction of nitrate over Pd based catalyst, *Appl. Catal. B: Environ.* 84 (2008) 156–161.

[39] Q. Wang, G. Li, B. Zhao, M. Shen, R. Zhou, The effect of La doping on the structure of Ce_{0.2}Zr_{0.8}O₂ and the catalytic performance of its supported Pd-only three-way catalyst, *Appl. Catal. B: Environ.* 101 (2010) 150–159.

[40] P. Kast, M. Friedrich, F. Girsidis, J. Kröhnert, D. Teschner, T. Lunkenstein, M. Behrens, R. Schlogl, Strong metal–support interaction and alloying in Pd/ZnO catalysts for CO oxidation, *Catal. Today* 260 (2016) 21–31.

[41] A. Baylet, P. Marecot, D. Duprez, P. Castellazzi, G. Groppi, P. Forzatti, In situ Raman and in situ XRD analysis of PdO reduction and Pd⁰ oxidation supported on γ -Al₂O₃ catalyst under different atmospheres, *Phys. Chem. Chem. Phys.* 13 (2011) 4607–4613.

[42] H. Zhu, Z. Qin, W. Shan, W. Shen, J. Wang, Pd/CeO₂–TiO₂ catalyst for CO oxidation at low temperature: a TPR study with H₂ and CO as reducing agents, *J. Catal.* 225 (2004) 267–277.

[43] N. Tsud, V. Johánek, I. Stará, K. Veltruská, V. Matolín, XPS, ISS and TPD study of Pd–Sn interactions on Pd–SnO_x systems, *Thin Solid Films* 391 (2001) 204–208.

[44] G. Boskovic, M. Kovacevic, E. Kiss, J. Radnik, M. Pohl, M. Schneider, U. Bentrup, A. Bruckner, Strong metal–support interaction as activity requirement of palladium-supported tin oxide sol–gel catalyst for water denitration, *Int. J. Environ. Sci. Technol.* 9 (2012) 235–246.

[45] G. Postole, M. Caldăraru, B. Bonnetot, A. Auroux, Influence of the support surface chemistry on the catalytic performances of PdO/BN catalysts, *J. Phys. Chem. C* 112 (2008) 11385–11393.

[46] B. Huber, H. Gnaser, C. Ziegler, Electrical properties of nanocrystalline anatase TiO₂ thin films with different crystallite size, *Surf. Sci.* 566–568 (Part 1) (2004) 419–424.

[47] L.-q. Mao, Q.-l. Li, Z.-j. Zhang, Study on surface states of Pt/TiO₂ thin film in different atmospheres, *Sol. Energy* 81 (2007) 1280–1284.

[48] M. Haruta, Gold as a novel catalyst in the 21st century: preparation, working mechanism and applications, *Gold Bull.* 37 (2004) 27–36.